A novel CpG-methylation-based nomogram predicts survival in colorectal cancer

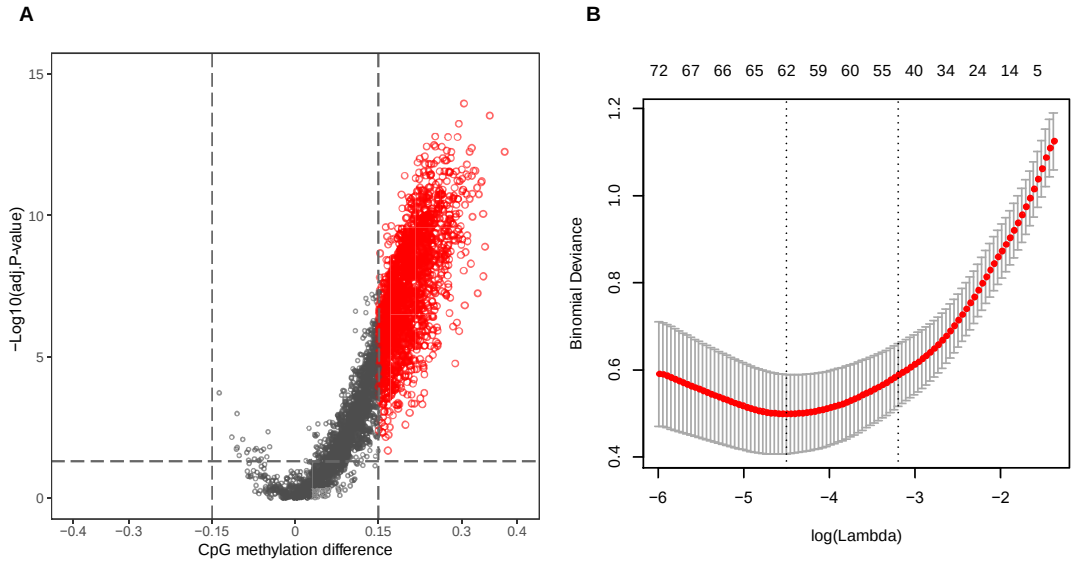

Supplementary Figure S1. Identification of 47 labeled CpGs in traning cohort. (**A**) Volcano plot of biological significance (CpG methylation difference) versus the statistical significance (–log10[adjusted *p* value]) showing 1526 differentially methylated CpGs (Wilcoxon rank test *p* value < 0.05 and |CpG methylation difference| > 0.15) between the two groups generated by the clustering. (**B**) Ten-fold cross-validation for LASSO logistical regression using the 1526 CpGs identified 47 labeled CpGs. The two dotted vertical lines are drawn at the optimal values by minimum criteria and 1-standard error criteria, respectively. A tuning parameter λ = 0.041 with log (λ) = -3.199 was chosen by 1-standard error criteria.

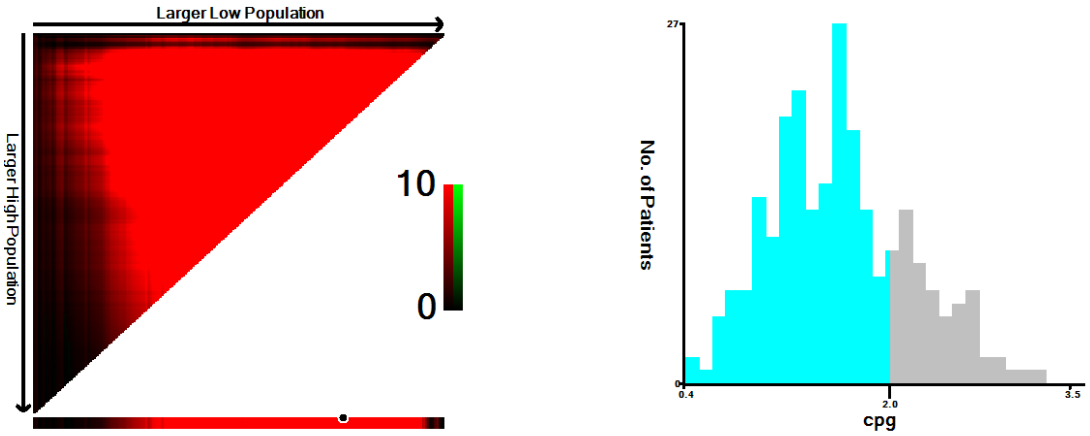

Supplementary Figure S2. The optimal cutoff of the risk score of the six-CpG signature was determined by the X-tile plots in training cohort. The dark dot in the X-tile plots represents the cutoff point based on the highest χ^2-value with Kaplan–Meier survival analysis to divide patients into two groups.

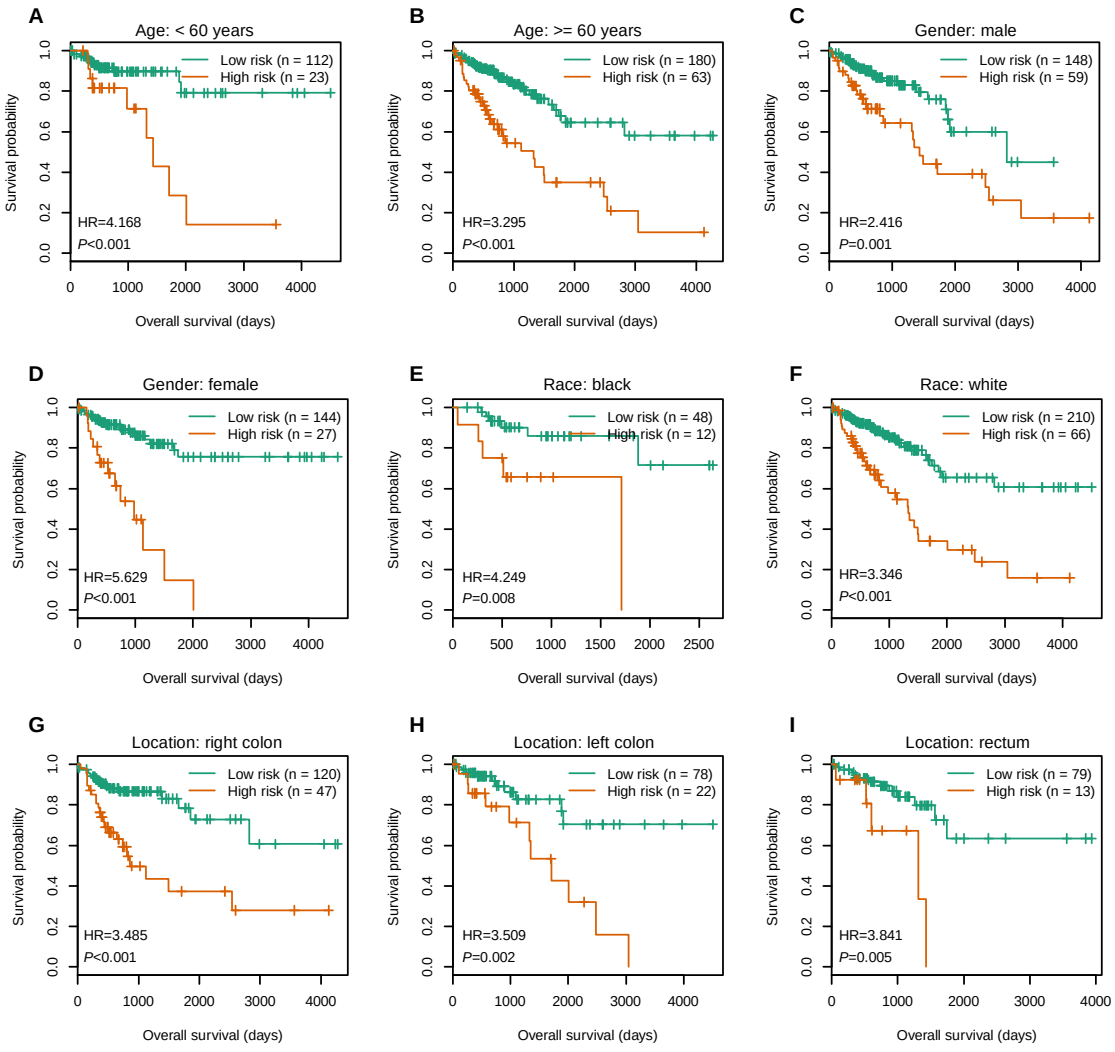

Supplementary Figure S3. Kaplan-Meier survival curves of the six-CpG signature in different subgroups stratified by clinicopathological characteristics. (**A, B**) Age, (**C, D**) Gender, (**E, F**) Race, (**G-I**) Location.

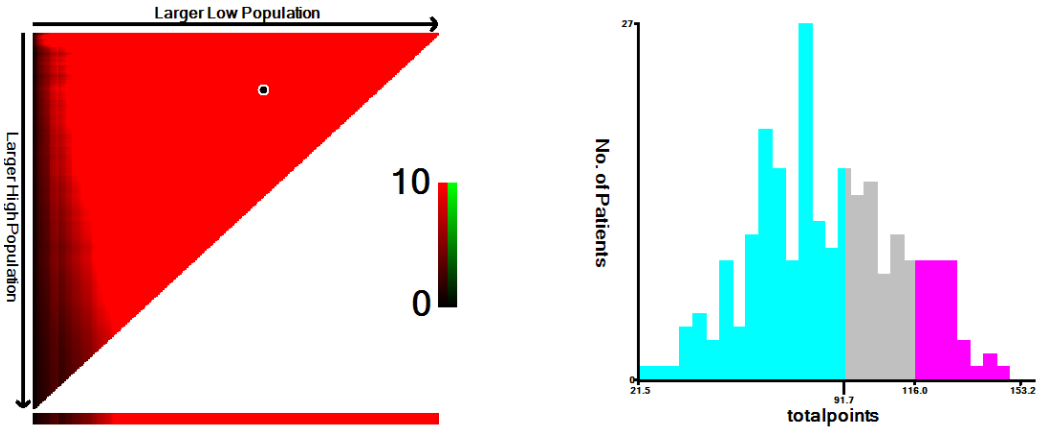

Supplementary Figure S4. The optimal cutoff of the total points of the nomogram was determined by the X-tile plots in training cohort. The dark dot in the X-tile plots represents the cutoff point based on the highest χ^2-value with Kaplan–Meier survival analysis to divide patients into three groups.

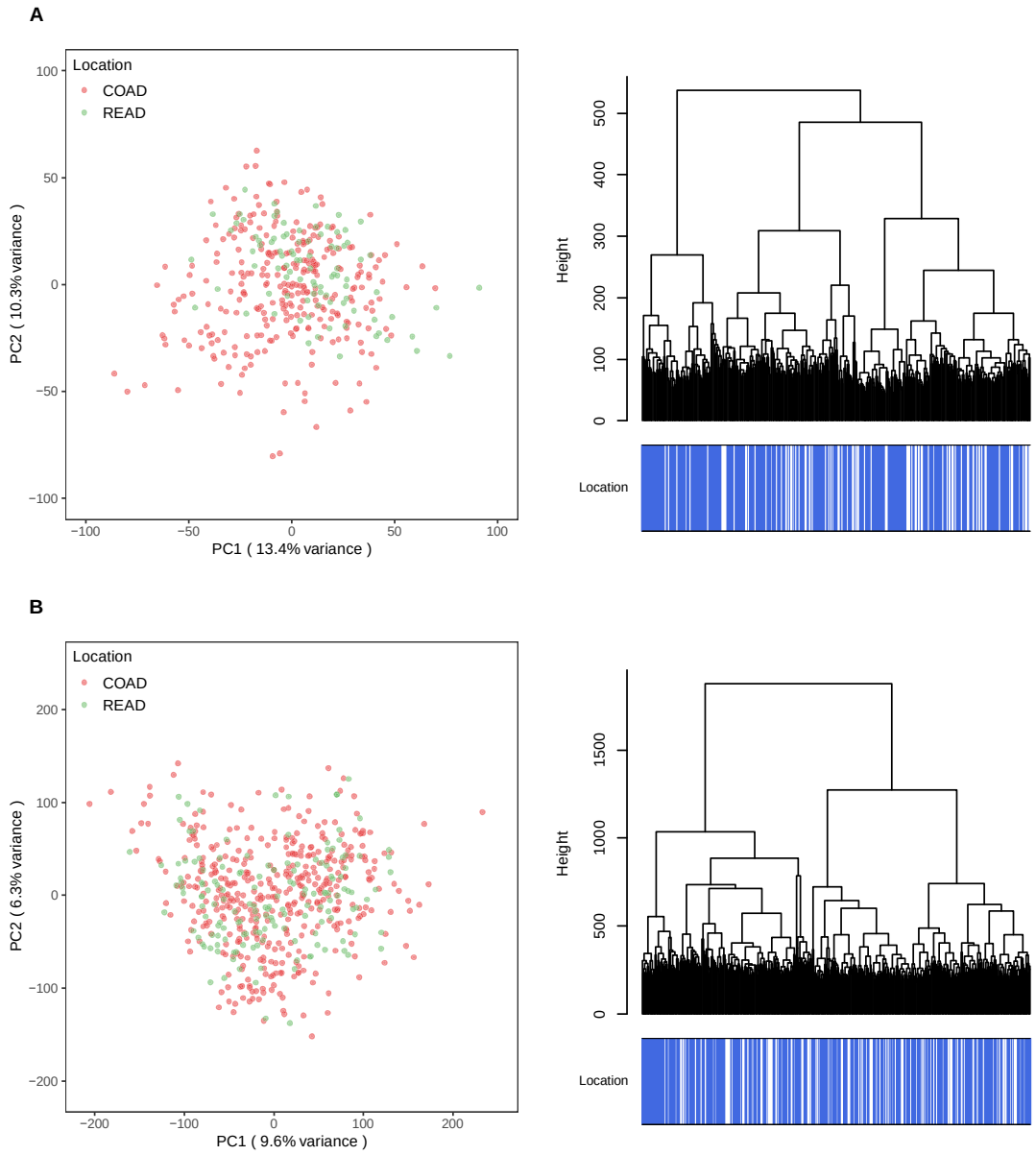

Supplementary Figure S5. Principal component analysis (left) and unsupervised hierarchical clustering (right) for methylation data (**A**) and gene expression data (**B**) of TCGA-COADREAD dataset, respectively.

Supplementary Table S1. Baseline characteristics of patients by the six-CpG signature.

Characteristic	Group	Training cohort (n=249)			Test cohort (n=129)		
		Number	Low risk (n=187, %)	High risk (n=62, %)	Number	Low risk (n=106, %)	High risk (n=23, %)
Age (years)	<60	89	74	15	46	38	8
	>= 60	160	112	48	83	68	15
Gender	Male	143	97	46	64	51	13
	Female	106	89	17	65	55	10
Race	Asian	7	3	4	5	3	2
	White	178	132	46	98	78	20
	Black	41	30	11	19	18	1
	American Indian	0	0	0	1	1	0
	Not available	23	21	2	6	6	0
T stage	T1	8	8	0	4	3	1
	T2	29	22	7	25	23	2
	T3	178	129	49	84	67	17
	T4	33	27	6	16	13	3
	Not available	1	0	1	0	0	0
N stage	N0	136	103	33	68	59	9
	N1	63	48	15	39	33	6
	N2	47	33	14	22	14	8
	Nx	2	2	0	0	0	0
	Not available	1	0	1	0	0	0
M stage	M0	206	153	53	107	88	19
	M1	34	26	8	20	16	4
	Mx	6	6	0	2	2	0
	Not available	3	1	2	0	0	0
TNM stage	I	32	25	7	23	20	3
	II	95	71	24	42	36	6
	III	79	57	22	42	32	10
	IV	34	26	8	20	16	4
	Not available	9	7	2	2	2	0
Location	Right colon	109	76	33	58	44	14
	Left colon	62	47	15	38	31	7
	Rectum	64	53	11	28	26	2
	Not available	14	10	4	5	5	0

Supplementary Table S2. Pathways enriched in six-CpG signature-defined high-risk group by GSEA (C2 gene sets, FDR < 0.05).

NAME	SIZE	ES	NES	NOM p-val	FDR q-val	FWER p-val
ROSTY_CERVICAL_CANCER_PROLIFERATION_CLUSTER	139	0.626	2.689	0.000	0.000	0.000
FISCHER_G2_M_CELL_CYCLE	232	0.558	2.619	0.000	0.000	0.000
KONG_E2F3_TARGETS	95	0.615	2.526	0.000	0.000	0.000
BENPORATH_PROLIFERATION	146	0.543	2.362	0.000	0.000	0.000
ZHOU_CELL_CYCLE_GENES_IN_IR_RESPONSE_6HR	82	0.602	2.359	0.000	0.000	0.001
PUJANA_BRCA_CENTERED_NETWORK	118	0.566	2.356	0.000	0.000	0.001
KOBAYASHI_EGFR_SIGNALING_24HR_DN	251	0.514	2.352	0.000	0.000	0.001
HOFFMANN_LARGE_TO_SMALL_PRE_BII_LYMPHOCYTE_UP	150	0.542	2.346	0.000	0.000	0.001
SARRIO_EPITHELIAL_MESENCHYMAL_TRANSITION_UP	178	0.534	2.325	0.000	0.000	0.001
WINNEPENNINCKX_MELANOMA_METASTASIS_UP	160	0.550	2.323	0.000	0.000	0.001
KANG_DOXORUBICIN_RESISTANCE_UP	54	0.641	2.311	0.000	0.000	0.001
SHEDDEN_LUNG_CANCER_POOR_SURVIVAL_A6	450	0.468	2.276	0.000	0.000	0.003
FARMER_BREAST_CANCER_CLUSTER_2	33	0.683	2.272	0.000	0.000	0.004
KAUFFMANN_DNA_REPAIR_GENES	226	0.492	2.236	0.000	0.001	0.005
DUTERTRE_ESTRADIOL_RESPONSE_24HR_UP	320	0.491	2.211	0.000	0.001	0.009
REICHERT_MITOSIS_LIN9_TARGETS	27	0.702	2.197	0.000	0.001	0.010
SENGUPTA_NASOPHARYNGEAL_CARCINOMA_UP	297	0.452	2.187	0.000	0.001	0.011
MORI_IMMATURE_B_LYMPHOCYTE_DN	89	0.537	2.163	0.000	0.001	0.015
TOYOTA_TARGETS_OF_MIR34B_AND_MIR34C	430	0.454	2.160	0.000	0.001	0.015
WHITFIELD_CELL_CYCLE_LITERATURE	42	0.621	2.157	0.000	0.001	0.015
CROONQUIST_NRAS_SIGNALING_DN	70	0.560	2.152	0.000	0.001	0.015
MISSIAGLIA_REGULATED_BY_METHYLATION_DN	117	0.525	2.150	0.000	0.001	0.016
KAMMINGA_EZH2_TARGETS	41	0.615	2.136	0.000	0.001	0.019
KAUFFMANN_MELANOMA_RELAPSE_UP	60	0.564	2.112	0.000	0.002	0.033
FUJII_YBX1_TARGETS_DN	190	0.478	2.112	0.000	0.002	0.033
VANTVEER_BREAST_CANCER_METASTASIS_DN	128	0.490	2.094	0.000	0.003	0.045
ZHOU_CELL_CYCLE_GENES_IN_IR_RESPONSE_24HR	122	0.499	2.085	0.000	0.003	0.056
MORI_EMU_MYC_LYMPHOMA_BY_ONSET_TIME_UP	108	0.509	2.084	0.000	0.003	0.056
CHEMNITZ_RESPONSE_TO_PROSTAGLANDIN_E2_UP	140	0.484	2.080	0.000	0.003	0.059
WHITEFORD_PEDIATRIC_CANCER_MARKERS	115	0.501	2.079	0.000	0.003	0.059
ISHIDA_E2F_TARGETS	53	0.568	2.076	0.000	0.003	0.062
UDAYAKUMAR_MED1_TARGETS_UP	131	0.487	2.074	0.000	0.003	0.065
PYEON_CANCER_HEAD_AND_NECK_VS_CERVICAL_UP	182	0.464	2.070	0.000	0.003	0.070
NIKOLSKY_BREAST_CANCER_5P15_AMPLICON	26	0.664	2.066	0.000	0.003	0.072
EGUCHI_CELL_CYCLE_RB1_TARGETS	23	0.668	2.062	0.000	0.003	0.075
FINETTI_BREAST_CANCER_KINOME_RED	16	0.756	2.056	0.000	0.003	0.082
ODONNELL_TFRC_TARGETS_DN	126	0.489	2.054	0.000	0.003	0.083
PUJANA_XPRSS_INT_NETWORK	167	0.471	2.050	0.000	0.004	0.088
REACTOME_MITOTIC_SPINDLE_CHECKPOINT	110	0.502	2.050	0.000	0.003	0.088
REACTOME_RESOLUTION_OF_D_LOOP_STRUCTURES_THROUGH_SYNTHESIS_DEPENDENT_	26	0.656	2.037	0.000	0.004	0.096

STRAND_ANNEALING_SDSA						
KOINUMA_COLON_CANCER_MSI_UP	16	0.747	2.031	0.000	0.004	0.100
MANALO_HYPOXIA_DN	289	0.441	2.030	0.000	0.004	0.101
BIDUS_METASTASIS_UP	214	0.452	2.023	0.000	0.004	0.107
PUJANA_BREAST_CANCER_WITH_BRCA1_MUTATED_UP	57	0.556	2.018	0.000	0.004	0.115
WAKASUGI_HAVE_ZNF143_BINDING_SITES	60	0.536	2.012	0.000	0.005	0.131
REACTOME_MITOTIC_PROMETAPHASE	198	0.452	2.011	0.000	0.005	0.132
MITSIADES_RESPONSE_TO_APLIDIN_DN	246	0.443	2.009	0.000	0.005	0.138
REACTOME_RRNA_PROCESSING_IN_THE_NUCLEUS_AND_CYTOSOL	192	0.438	2.002	0.000	0.005	0.147
FRASOR_RESPONSE_TO_SERM_OR_FULVESTRANT_DN	48	0.571	2.001	0.000	0.005	0.150
MOREAUX_MULTIPLE_MYELOMA_BY_TACI_DN	173	0.452	2.000	0.000	0.005	0.150
CROONQUIST_IL6_DEPRIVATION_DN	95	0.490	1.999	0.000	0.005	0.152
ZHAN_MULTIPLE_MYELOMA_PR_UP	46	0.571	1.992	0.000	0.005	0.164
REACTOME_ACTIVATION_OF_THE_MRNA_UPON_BINDING_OF_THE_CAP_BINDING_COMPLEX_ AND_EIFS_AND_SUBSEQUENT_BINDING_TO_43S	60	0.541	1.992	0.000	0.005	0.165
MOLENAAR_TARGETS_OF_CCND1_AND_CDK4_DN	57	0.539	1.985	0.000	0.005	0.177
FLORIO_NEOCORTEX_BASAL_RADIAL_GLIA_DN	188	0.448	1.977	0.000	0.006	0.196
REACTOME_HDR_THROUGH_HOMOLOGOUS_RECOMBINATION_HRR	67	0.518	1.972	0.000	0.006	0.210
VECCHI_GASTRIC_CANCER_EARLY_UP	415	0.401	1.971	0.000	0.006	0.213
KEGG_HOMOLOGOUS_RECOMBINATION	28	0.609	1.971	0.004	0.006	0.214
MORI_LARGE_PRE_BII_LYMPHOCYTE_UP	84	0.495	1.967	0.000	0.006	0.224
YU_MYC_TARGETS_UP	42	0.574	1.964	0.000	0.007	0.239
REACTOME_RRNA_PROCESSING	202	0.436	1.959	0.000	0.007	0.255
CHIANG_LIVER_CANCER_SUBCLASS_PROLIFERATION_UP	175	0.438	1.959	0.000	0.007	0.255
RHODES_UNDIFFERENTIATED_CANCER	68	0.501	1.957	0.000	0.007	0.258
REACTOME_PROCESSING_OF_CAPPED_INTRON_CONTAINING_PRE_MRNA	241	0.424	1.957	0.000	0.007	0.258
WU_APOPTOSIS_BY_CDKN1A_VIA_TP53	51	0.544	1.955	0.000	0.007	0.262
BILANGES_SERUM_SENSITIVE_VIA_TSC2	29	0.604	1.953	0.000	0.007	0.270
REACTOME_SUMOYLATION_OF_RNA_BINDING_PROTEINS	47	0.546	1.951	0.000	0.007	0.273
REACTOME_SUMOYLATION_OF_DNA_METHYLATION_PROTEINS	16	0.712	1.950	0.000	0.007	0.277
REACTOME_HOMOLOGOUS_DNA_PAIRING_AND_STRAND_EXCHANGE	42	0.568	1.950	0.000	0.007	0.282
REACTOME_RNA_POLYMERASE_I_TRANSCRIPTION_TERMINATION	31	0.594	1.948	0.000	0.007	0.285
HORIUCHI_WTAP_TARGETS_DN	309	0.414	1.947	0.000	0.007	0.291
BILANGES_SERUM_AND_RAPAMYCIN_SENSITIVE_GENES	50	0.541	1.938	0.000	0.008	0.324
BOYAULT_LIVER_CANCER_SUBCLASS_G3_UP	190	0.438	1.937	0.000	0.008	0.324
FOURNIER_ACINAR_DEVELOPMENT_LATE_2	281	0.415	1.924	0.000	0.009	0.365
REACTOME_RESOLUTION_OF_D_LOOP_STRUCTURES	34	0.585	1.922	0.000	0.009	0.370
PID_FANCONI_PATHWAY	47	0.544	1.921	0.000	0.009	0.373
REACTOME_SUMOYLATION_OF_DNA_REPLICATION_PROTEINS	46	0.532	1.918	0.000	0.009	0.383
REACTOME_SUMOYLATION_OF_DNA_DAMAGE_RESPONSE_AND_REPAIR_PROTEINS	77	0.482	1.918	0.000	0.009	0.384
KEGG_RIBOSOME	86	0.483	1.913	0.000	0.010	0.406
WONG_EMBRYONIC_STEM_CELL_CORE	333	0.409	1.904	0.000	0.011	0.442
REACTOME_GLOBAL_GENOME_NUCLEOTIDE_EXCISION_REPAIR_GG_NER	84	0.482	1.894	0.000	0.012	0.486

REACTOME_EUKARYOTIC_TRANSLATION_INITIATION	119	0.456	1.894	0.000	0.012	0.486
YUAN_ZNF143_PARTNERS	22	0.625	1.891	0.000	0.012	0.502
SONG_TARGETS_OF_IE86_CMV_PROTEIN	54	0.526	1.889	0.000	0.012	0.503
LI_WILMS_TUMOR_VS_FETAL_KIDNEY_1_DN	161	0.433	1.885	0.000	0.013	0.525
IRITANI_MAD1_TARGETS_DN	41	0.532	1.884	0.000	0.013	0.527
REACTOME_RNA_POLYMERASE_II_TRANSCRIPTION_TERMINATION	66	0.489	1.883	0.006	0.013	0.527
REACTOME_ACTIVATION_OF_THE_PRE_REPLICATIVE_COMPLEX	33	0.565	1.883	0.004	0.013	0.527
REACTOME_RESOLUTION_OF_SISTER_CHROMATID_COHESION	125	0.444	1.880	0.000	0.013	0.544
REACTOME_MRNA_SPLICING	187	0.422	1.877	0.000	0.014	0.562
REACTOME_NUCLEOTIDE_EXCISION_REPAIR	110	0.458	1.876	0.000	0.014	0.564
THILLAINADESAN_ZNF217_TARGETS_UP	40	0.542	1.868	0.000	0.015	0.605
VERNELL_RETINOBLASTOMA_PATHWAY_UP	70	0.476	1.861	0.000	0.016	0.631
REACTOME_RNA_POLYMERASE_II_TRANSCRIPTION_PRE_INITIATION_AND_PROMOTER_OPENING	47	0.508	1.856	0.000	0.016	0.650
REACTOME_SRP_DEPENDENT_COTRANSLATIONAL_PROTEIN_TARGETING_TO_MEMBRANE	112	0.445	1.848	0.000	0.017	0.678
WATANABE_COLON_CANCER_MSI_VS_MSS_UP	28	0.586	1.845	0.007	0.018	0.688
BURTON_ADIPOGENESIS_PEAK_AT_24HR	44	0.521	1.844	0.000	0.018	0.691
REACTOME_RNA_POLYMERASE_II_PRE_TRANSCRIPTION_EVENTS	84	0.460	1.843	0.000	0.018	0.692
DANG_MYC_TARGETS_UP	128	0.443	1.839	0.000	0.019	0.711
REACTOME_SUMOYLATION_OF_UBIQUITINYLATION_PROTEINS	39	0.528	1.838	0.000	0.019	0.717
REACTOME_SUMOYLATION_OF_TRANSCRIPTION_FACTORS	20	0.631	1.837	0.000	0.019	0.720
MARKEY_RB1_ACUTE_LOF_UP	229	0.392	1.836	0.000	0.019	0.721
PID_BARD1_PATHWAY	29	0.580	1.834	0.000	0.019	0.734
WHITFIELD_CELL_CYCLE_S	147	0.428	1.833	0.000	0.019	0.734
REACTOME_TRANSLATION	292	0.390	1.833	0.000	0.019	0.736
XU_HGF_SIGNALING_NOT_VIA_AKT1_48HR_DN	18	0.658	1.831	0.000	0.019	0.744
REACTOME_TRANSPORT_OF_MATURE_MRNAS_DERIVED_FROM_INTRONLESS_TRANSCRIPTS	43	0.524	1.824	0.004	0.020	0.769
REACTOME_TRANSPORT_OF_MATURE_TRANSCRIPT_TO_CYTOPLASM	84	0.460	1.822	0.000	0.021	0.776
REACTOME_TRANSCRIPTIONAL_REGULATION_BY_E2F6	34	0.547	1.820	0.000	0.021	0.785
REACTOME_RNA_POLYMERASE_II_TRANSCRIBES_SNRNA_GENES	74	0.468	1.820	0.000	0.021	0.785
SCHLOSSER_MYC_TARGETS_REPRESSED_BY_SERUM	159	0.420	1.820	0.000	0.021	0.787
REACTOME_TRANSCRIPTION_OF_THE_HIV_GENOME	73	0.464	1.818	0.000	0.021	0.797
REACTOME_G1_S_SPECIFIC_TRANSCRIPTION	29	0.580	1.815	0.004	0.021	0.808
REACTOME_HDR_THROUGH_SINGLE_STRAND_ANNEALING_SSA	37	0.529	1.813	0.004	0.021	0.812
PID_FOXM1_PATHWAY	40	0.525	1.807	0.004	0.023	0.836
REACTOME_FORMATION_OF_INCISION_COMPLEX_IN_GG_NER	43	0.513	1.807	0.009	0.022	0.836
REACTOME_TRNA_PROCESSING_IN_THE_NUCLEUS	58	0.479	1.807	0.000	0.022	0.836
KEGG_RNA_DEGRADATION	56	0.483	1.807	0.000	0.022	0.836
REACTOME_S_PHASE	161	0.412	1.802	0.000	0.023	0.858
REACTOME_ANCHORING_OF_THE_BASAL_BODY_TO_THE_PLASMA_MEMBRANE	96	0.447	1.802	0.000	0.023	0.859
REN_BOUND_BY_E2F	61	0.468	1.800	0.000	0.023	0.863
FERREIRA_EWINGS_SARCOMA_UNSTABLE_VS_STABLE_UP	160	0.419	1.799	0.000	0.024	0.867
REACTOME_INFLUENZA_INFECTION	155	0.410	1.796	0.000	0.024	0.872
WEST_ADRENOCORTICAL_TUMOR_MARKERS_UP	22	0.589	1.796	0.003	0.024	0.873

RHODES_CANCER_META_SIGNATURE	65	0.476	1.795	0.000	0.024	0.876
PID_ATM_PATHWAY	34	0.538	1.794	0.000	0.024	0.880
KEGG_NUCLEOTIDE_EXCISION_REPAIR	44	0.505	1.794	0.000	0.024	0.881
KEGG_CELL_CYCLE	124	0.434	1.789	0.000	0.025	0.892
NAKAMURA_CANCER_MICROENVIRONMENT_DN	45	0.510	1.787	0.000	0.025	0.900
ABRAMSON_INTERACT_WITH_AIRE	45	0.511	1.784	0.000	0.025	0.908
SCHLOSSER_MYC_TARGETS_AND_SERUM_RESPONSE_UP	46	0.502	1.783	0.000	0.026	0.911
REACTOME_RHO_GTPASES_ACTIVATE_FORMINS	139	0.412	1.781	0.000	0.026	0.914
BURTON_ADIPOGENESIS_3	100	0.434	1.779	0.000	0.026	0.917
REACTOME_INTERACTIONS_OF_VPR_WITH_HOST_CELLULAR_PROTEINS	37	0.518	1.777	0.004	0.026	0.923
MOREAUX_B_LYMPHOCYTE_MATURATION_BY_TACI_DN	76	0.457	1.775	0.000	0.027	0.924
STEIN_ESRRA_TARGETS_RESPONSIVE_TO_ESTROGEN_DN	41	0.498	1.775	0.000	0.027	0.924
PYEON_HPV_POSITIVE_TUMORS_UP	90	0.445	1.771	0.000	0.027	0.929
REACTOME_SUMOYLATION_OF_SUMOYLATION_PROTEINS	35	0.523	1.767	0.008	0.028	0.935
REACTOME_RNA_POLYMERASE_I_TRANSCRIPTION_INITIATION	47	0.506	1.765	0.005	0.028	0.939
REACTOME_INTERACTIONS_OF_REV_WITH_HOST_CELLULAR_PROTEINS	37	0.528	1.765	0.008	0.028	0.939
ODONNELL_TARGETS_OF_MYC_AND_TFRC_DN	45	0.489	1.759	0.000	0.030	0.950
REACTOME_ACTIVATION_OF_ATR_IN_RESPONSE_TO_REPLICATION_STRESS	37	0.527	1.759	0.000	0.029	0.950
LI_WILMS_TUMOR_ANAPLASTIC_UP	17	0.634	1.759	0.019	0.029	0.950
REACTOME_TRANSCRIPTION_COUPLED_NUCLEOTIDE_EXCISION_REPAIR_TC_NER	78	0.453	1.756	0.000	0.030	0.951
REACTOME_NUCLEAR_IMPORT_OF_REV_PROTEIN	34	0.523	1.756	0.000	0.030	0.951
BIOCARTA_G1_PATHWAY	28	0.546	1.752	0.004	0.030	0.953
PID_MYC_ACTIV_PATHWAY	79	0.435	1.751	0.000	0.031	0.954
REACTOME_RNA_POLYMERASE_III_TRANSCRIPTION	41	0.505	1.748	0.004	0.031	0.960
REACTOME_NONSENSE_MEDIATED_DECAY_NMD	115	0.413	1.747	0.000	0.031	0.961
REACTOME_MITOTIC_G1_G1_S_PHASES	149	0.401	1.746	0.000	0.031	0.963
GARGALOVIC_RESPONSE_TO_OXIDIZED_PHOSPHOLIPIDS_RED_UP	15	0.646	1.741	0.003	0.033	0.968
PID_AURORA_A_PATHWAY	31	0.537	1.736	0.000	0.034	0.973
REACTOME_TRANSPORT_OF_THE_SLBP_DEPENDANT_MATURE_MRNA	36	0.514	1.734	0.000	0.035	0.974
REACTOME_NUCLEAR_PORE_COMPLEX_NPC_DISASSEMBLY	36	0.509	1.726	0.004	0.037	0.981
REACTOME_DNA_STRAND_ELONGATION	32	0.517	1.726	0.007	0.037	0.981
LY_AGING_MIDDLE_DN	15	0.620	1.720	0.006	0.039	0.985
REACTOME_CENTROSOME_MATURATION	81	0.427	1.716	0.000	0.040	0.989
WHITFIELD_CELL_CYCLE_G2	163	0.397	1.715	0.000	0.040	0.989
FURUKAWA_DUSP6_TARGETS_PCI35_DN	69	0.456	1.714	0.006	0.040	0.990
PID_AURORA_B_PATHWAY	37	0.514	1.712	0.000	0.041	0.990
GRAHAM_NORMAL_QUIESCENT_VS_NORMAL_DIVIDING_DN	89	0.424	1.712	0.000	0.041	0.990
WHITFIELD_CELL_CYCLE_M_G1	128	0.405	1.711	0.000	0.041	0.990
REACTOME_CYCLIN_A_B1_B2_ASSOCIATED_EVENTS_DURING_G2_M_TRANSITION	25	0.557	1.708	0.003	0.041	0.990
REACTOME_NONSENSE_MEDIATED_DECAY_NMD_INDEPENDENT_OF_THE_EXON_JUNCTION_COMPLEX_EJC	95	0.407	1.705	0.000	0.042	0.992
REACTOME_AURKA_ACTIVATION_BY_TPX2	72	0.436	1.700	0.000	0.044	0.993
YAO_TEMPORAL_RESPONSE_TO_PROGESTERONE_CLUSTER_10	69	0.444	1.699	0.000	0.044	0.993
NIKOLSKY_BREAST_CANCER_15Q26_AMPLICON	21	0.558	1.695	0.006	0.045	0.994

FARMER_BREAST_CANCER_CLUSTER_5	19	0.592	1.693	0.027	0.046	0.994
SCIAN_CELL_CYCLE_TARGETS_OF_TP53_AND_TP73_DN	21	0.566	1.692	0.011	0.046	0.997
TANG_SENESCENCE_TP53_TARGETS_DN	55	0.460	1.688	0.000	0.047	0.997
REACTOME_CELL_CYCLE_CHECKPOINTS	291	0.356	1.687	0.000	0.048	0.997
REACTOME_MITOTIC_METAPHASE_AND_ANAPHASE	201	0.378	1.685	0.000	0.048	0.998
REACTOME_REGULATION_OF_TP53_ACTIVITY_THROUGH_PHOSPHORYLATION	92	0.420	1.681	0.000	0.049	0.998

Supplementary Table S3. Previously published methylation markers for prognostic prediction of colorectal cancer.

Signature	CpG site
Five CpGs of Jia et al.	cg02425108, cg08044454, cg15659052, cg16935707, cg24311416
19 CpGs from Gündert et al.	cg00832644, cg05646575, cg08617020, cg08729279, cg08804626, cg10758824, cg11056055, cg12510999, cg14270346, cg14983135, cg16336556, cg16399624, cg17431888, cg18195165, cg18736676, cg19184885, cg19340296, cg22522598, cg23750514